Neuro-Oncology

23(3), 387–399, 2021 | doi:10.1093/neuonc/noaa255 | Advance Access date 3 November 2020

PTRF/cavin-1 remodels phospholipid metabolism to promote tumor proliferation and suppress immune responses in glioblastoma by stabilizing cPLA2

Kaikai Yi,† Qi Zhan,† Qixue Wang, Yanli Tan, Chuan Fang, Yunfei Wang, Junhu Zhou, Chao Yang, Yansheng Li, and Chunsheng Kang

Laboratory of Neuro-oncology, Tianjin Neurological Institute, Department of Neurosurgery, Tianjin Medical University General Hospital, Key Laboratory of Post-Neuro Injury Neuro-repair and Regeneration in Central Nervous System, Ministry of Education and Tianjin City, Tianjin, China (K.Y., Q.W., Y.W., J.Z., C.Y., Y.L., C.K.); Tianjin Key Laboratory of Composite and Functional Materials, School of Material Science and Engineering, Tianjin University, Tianjin China (Q.Z.); Department of Pathology, Affiliated Hospital of Hebei University, Baoding, China (Y.T.); Department of Neurosurgery, Affiliated Hospital of Hebei University, Baoding, China (C.F.); Department of Pathology, Hebei University Medical College, Baoding, China (Y.T.)

Corresponding Author: Chunsheng Kang, Tianjin Medical University General Hospital, 154 Anshan Road, Tianjin 300052, China (kang97061@tmu.edu.cn).

†Kaikai Yi and Qi Zhan contributed equally to this work.

Abstract

Background. Metabolism remodeling is a hallmark of glioblastoma (GBM) that regulates tumor proliferation and the immune microenvironment. Previous studies have reported that increased polymerase 1 and transcript release factor (PTRF) levels are associated with a worse prognosis in glioma patients. However, the biological role and the molecular mechanism of PTRF in GBM metabolism remain unclear.

Methods. The relationship between PTRF and lipid metabolism in GBM was detected by nontargeted metabolomics profiling and subsequent lipidomics analysis. Western blotting, quantitative real-time PCR, and immunoprecipitation were conducted to explore the molecular mechanism of PTRF in lipid metabolism. A sequence of in vitro and in vivo experiments (both xenograft tumor and intracranial tumor mouse models) were used to detect the tumor-specific impacts of PTRF.

Results. Here, we show that PTRF triggers a cytoplasmic phospholipase A2 (cPLA2)–mediated phospholipid remodeling pathway that promotes GBM tumor proliferation and suppresses tumor immune responses. Research in primary cell lines from GBM patients revealed that cells overexpressing PTRF show increased cPLA2 activity—resulting from increased protein stability—and exhibit remodeled phospholipid composition. Subsequent experiments revealed that PTRF overexpression alters the endocytosis capacity and energy metabolism of GBM cells. Finally, in GBM xenograft and intracranial tumor mouse models, we showed that inhibiting cPLA2 activity blocks tumor proliferation and prevents PTRF-induced reduction in CD8+ tumor-infiltrating lymphocytes.

Conclusions. The PTRF-cPLA2 lipid remodeling pathway promotes tumor proliferation and suppresses immune responses in GBM. In addition, our findings highlight multiple new therapeutic targets for GBM.

Key Points

1. PTRF reprograms phospholipid metabolism by regulating the stability of cPLA2.
2. The PTRF-cPLA2 lipid remodeling pathway promotes tumor proliferation and suppresses immune responses, indicating new therapeutic targets for GBM.

Importance of the Study

Metabolic reprogramming is a hallmark of tumors and especially glioblastomas, and such reprogramming is known to be foundational for diverse pathomechanisms driving tumorigenicity and malignancy. Here, we found that PTRF remodels phospholipids by regulating cPLA2 protein stability and enhancing cPLA2 activity, which then promotes endocytosis and energy metabolism, intrinsically promotes tumor proliferation, and suppresses the immune response in GBM. Moreover, a cPLA2 inhibitor (AACOCF3) and metformin can reverse the role of the PTRF-cPLA2 lipid remodeling pathway in GBM. These findings highlight the supportive role of phospholipid metabolism in GBM, providing new therapeutic targets and immunotherapy strategies for further investigation.

Glioblastoma (GBM) is the most common primary brain tumor in adults.[1] Despite a standard treatment regimen that includes surgery combined with temozolomide chemotherapy and radiation therapy, patients still have a median survival of 12–16 months after initial diagnosis.[2] There is an urgent need to further understand the underlying mechanisms that promote tumor growth and survival, which will provide new targets for the treatment of GBM. Previous investigations have identified metabolic reprogramming as a major characteristic of GBM, which is related to proliferation and the immune microenvironment.[3,4]

Cancer metabolism provides enough energy to drive new biomass and active cell proliferation.[5] In addition to constituting the lipid bilayer structure of cell membranes, phospholipids are now understood to regulate a variety of cellular biological functions.[6] It is well documented that remodeling of the phospholipid content of membranes and cells has functional impacts on tumors.[7,8] In glioma, dramatic alterations in phospholipid composition have been observed in the isocitrate dehydrogenase mutation subtype.[9] Despite this growing appreciation of how phospholipid remodeling impacts many aspects of tumor biology, the roles and mechanisms of phospholipid remodeling in GBM are unclear.

Polymerase 1 and transcript release factor (PTRF), also known as cavin-1, is a conserved cytoplasmic protein that regulates caveola structure and function.[10] Previous studies have found that PTRF-knockout mice have higher levels of triglycerides in circulating blood but have significantly reduced adipose tissue.[11] The pathogenic effects of PTRF dysregulation have been validated in congenital generalized lipodystrophies, supporting the hypothesis that PTRF somehow regulates the synthesis of phospholipids and triglycerides.[12] In glioma, PTRF alters the tumor microenvironment by increasing exosome secretion,[13] and is associated with methylation regulation,[14] cell growth,[15] and the immune response,[16] thus it exerts a tumor-promoting function. However, the exact mechanism by which PTRF affects GBM metabolism remains unclear and needs further study.

Here, we built on our previous work showing that increased levels of PTRF are associated with a worse prognosis in glioma patients.[13] We found that PTRF-triggered lipid remodeling is mediated by cytoplasmic phospholipase A2 (cPLA2), and we showed that PTRF overexpression increases the enzymatic activity of cPLA2 by promoting its protein stability in GBM cells. A sequence of in vitro and in vivo experiments characterizing the broader physiological and tumor-specific impacts of this pathway revealed that elevated PTRF-cPLA2 lipid remodeling promotes endocytosis capacity, energy metabolism, and tumor-specific accumulation of adenosine.

Materials and Methods

Cell Culture, Lentiviruses, and Chemicals

The GL261 cell line was cultured in DMEM supplemented with 10% fetal bovine serum (FBS). Primary cell lines (N9, N33, and TBD0220) were cultured in DMEM/F12 with 10% FBS. Lentiviruses encoding the PTRF-enhanced green fluorescent protein (EGFP) fusion protein and luciferase were purchased from Genechem. Small interfering RNAs targeting PTRF were synthesized by GenePharma. pENTER-PTRF^{WT}-Flag plasmid was purchased from Vigene Biosciences. See the Supplementary Material for details.

Colony Formation Assay and Cell Viability Assay

For the colony formation assay, 300 cells were seeded in 6-well plates and cultured for 2 weeks. Colonies were fixed with 4% paraformaldehyde and stained with crystal violet. Plated were 2×10^3 cells in 96-well plates, and the Cell Counting Kit 8 assay was employed to evaluate cell viability. The proliferation rate of cells was detected based on the manufacturer's instructions at 24 and 48 h, respectively.

Analyses of Cellular Endocytosis Capacity

Confocal laser scanning microscopy (CLSM) and flow cytometry were used to study the endocytic capacity of GBM cells. Bovine serum albumin (BSA) was labeled with cyanine-5 (Cy5) (Cy5-E SE, US Everbright). N9 and N33 cells transduced with vector or PTRF were co-incubated with Cy5-BSA under normal cell culture conditions. After incubation, the cells were used for CLSM and flow cytometry analyses. See the Supplementary Material for details.

Western Blot Analysis and Immunoprecipitation

Protein was extracted from cells with radioimmunoprecipitation lysis buffer (Solarbio)

containing freshly added protease inhibitor cocktail (Solarbio) and phenylmethylsulfonyl fluoride. Then, 30 μg of protein was subjected to sodium dodecyl sulfate–polyacrylamide gel electrophoresis and transferred to polyvinylidene fluoride membranes. The membranes were incubated with primary antibodies, and then with secondary antibodies. Chemiluminescence detection was performed using G:BOXF3 (Syngene). For co-immunoprecipitation analysis, the cells were lysed and then incubated with Protein A/G Plus-Agarose (Santa Cruz Biotechnology) and cPLA2 antibodies (Cell Signaling Technology). After washing the sample 5 times with an immunoprecipitation lysis buffer, western blot analysis was performed. See the Supplementary Material for details.

Hematoxylin/Eosin and Immunohistochemical Staining

Paraffin-embedded tissue sections were used for hematoxylin and eosin (HE) staining. For immunohistochemistry (IHC) staining, tissue sections were dewaxed, hydrated, and antigen repaired. Tissue sections were incubated with the appropriate primary antibodies, and then with horseradish peroxidase–conjugated secondary antibodies. After DAB (3,3′-diaminobenzidine) was developed, the sections were observed with a microscope. See the Supplementary Material for details.

Seahorse Xfe Extracellular Flux Analysis (Mito Stress Test)

Cells were seeded on Seahorse XF24 cell culture microplates. Measurements of oxygen consumption rate (OCR) were performed according to the manufacturer's protocol. Extracellular flux experiments were performed on a Seahorse XF24 Analyzer (Seahorse Bioscience). See the Supplementary Material for details.

Fluorescence Recovery After Photobleaching Membrane Fluidity Assay

We incubated the cells with DiI (Sigma), and then washed the cells with phosphate buffered saline. For CLSM, we photobleached a limited area (~1 × 1 cm^2) of the marking film with a 100% laser pulse. After photobleaching, the fluorescence intensity was recorded every 10 seconds for 5 minutes. After background normalization, changes in fluorescence intensity were plotted over time to generate a fluorescence recovery after photobleaching (FRAP) curve. See the Supplementary Material for details.

In Vivo Intracranial Patient-Derived Xenograft Model

All in vivo experiments were conducted in accordance with animal protocols approved by the Institutional Animal Care and Use Committee at Tianjin Medical University. BALB/C nude mice were used to establish intracranial GBM patient-derived xenografts (PDX). The PDX model was derived from GBM patients undergoing surgery at Hebei University Affiliated Hospital. Tumor tissue was removed from the PDX model and processed into a single cell suspension. The cells were incubated with the PTRF overexpression construct, and then were injected into the mice. Bioluminescence imaging was used to detect intracranial tumor growth on days 7, 14, and 21. On day 21, the mice were sacrificed, and their brain tissues were fixed in 10% formalin. A Kaplan–Meier survival curve was completed in another bath of animal experiment and was only used to observe the animal's survival condition. See the Supplementary Material for details.

Gene Ontology Analysis, Gene Set Enrichment Analysis, and Single-Cell RNA Sequencing Analysis

The glioblastoma dataset was downloaded from The Cancer Genome Atlas (TCGA). Gene Ontology analysis was performed in DAVID (Database for Annotation, Visualization and Integrated Discovery) (https://david.ncifcrf.gov/). Gene set enrichment analysis (GSEA) was performed using GSEA software (https://www.gsea-msigdb.org/). Single-cell RNA sequencing analysis was performed with the online tool Single Cell Portal (http://singlecell.broadinstitute.org).

Statistics

All statistical analyses were performed using GraphPad Prism 8.0 software. Student's *t*-test was used to compare 2 experimental groups, and 1-way or 2-way ANOVA was used to compare 3 or more experimental groups. All data represent mean ± SD. Significance was defined as $*P < 0.05$, $**P < 0.01$, $***P < 0.001$, $****P < 0.0001$, ns = not significant.

Results

PTRF Increases Lysophosphatidylcholine Levels in GBM

In the present study, we considered the multiple lipid-regulating roles of PTRF. First, we investigated metabolic reprogramming in GBM. To determine whether PTRF is involved in metabolic remodeling in GBM, we successfully established primary GBM cell lines, and then used a lentivirus vector to overexpress a PTRF–enhanced green fluorescent protein (EGFP) fusion protein. We confirmed successful establishment of N9 and N33 GBM cells with strong PTRF-EGFP expression (N9 PTRF and N33 PTRF) (Supplementary Figure 1A). We then used liquid chromatography–mass spectrometry (LC-MS) to study the effect of PTRF on GBM cell metabolism (Figure 1A). First, we used a nontargeted metabolomics approach to measure the effects of increased PTRF levels on metabolites and identified 296 differentially accumulated known metabolites in N9 PTRF cells compared with N9 cells.

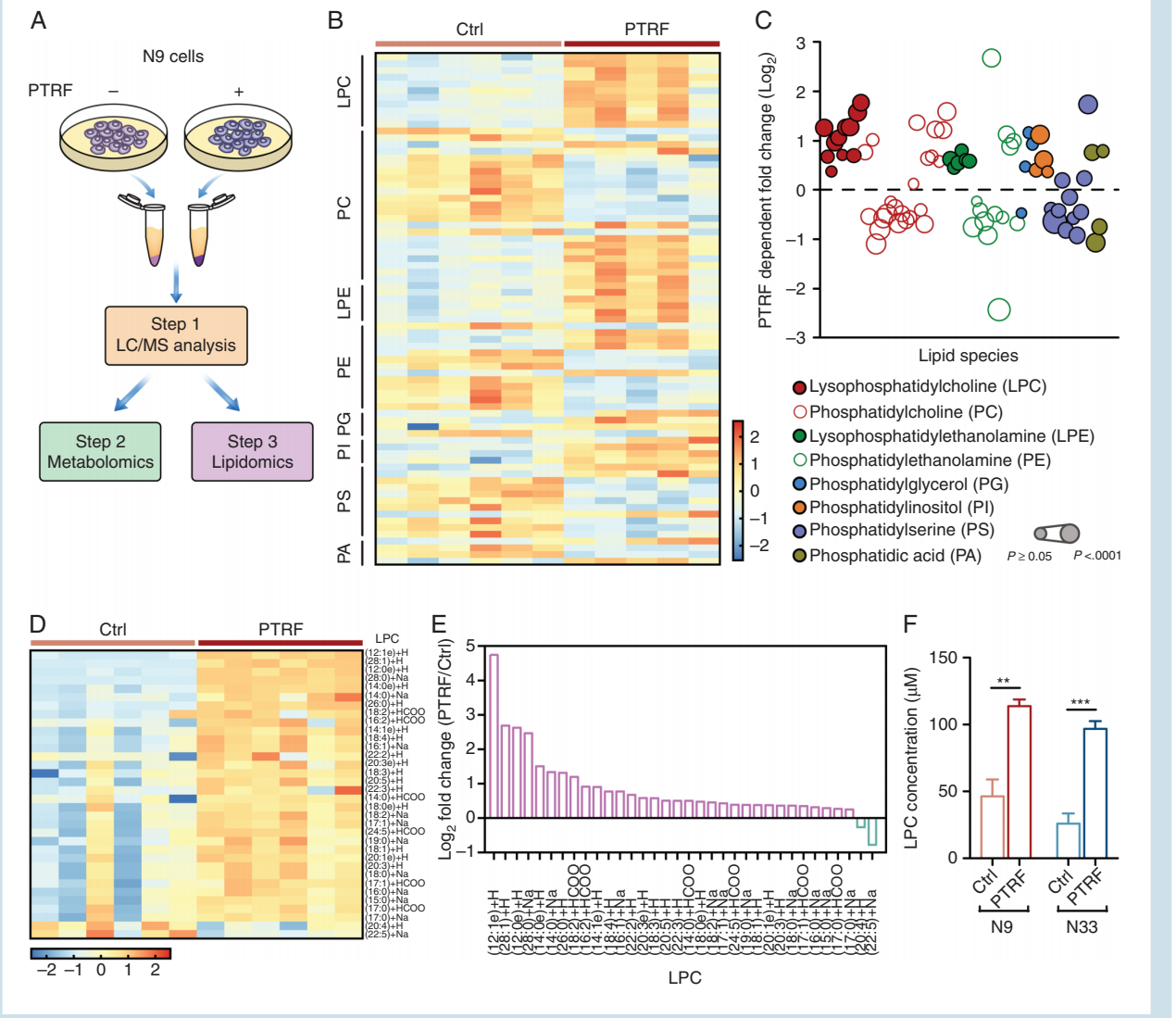

Fig. 1 PTRF increases lysophosphatidylcholine (LPC) levels in GBM. (A) Schematic of LC-MS analysis to study metabolism in primary GBM cells with or without PTRF overexpression. (B) Heatmap of phospholipid changes in N9 and N9 PTRF cells as assessed via nontargeted metabolomics analysis. Control group: $n = 6$; PTRF overexpression group: $n = 5$. (C) Nontargeted metabolomics analysis of phospholipids in N9 and N9 PTRF cells. Values are shown as $\log_2$ fold change relative to N9 cells. (D) Heatmap of lysophosphatidylcholine changes in N9 and N9 PTRF cells by lipidomics analysis. $n = 6$ for both groups. (E) Fold changes in the levels of various lysophosphatidylcholines in N9 and N9 PTRF cells. (F) ELISA-based analysis of total LPC levels in GBM cells.

It was interesting that approximately 55% of the differentially accumulated metabolites were lipids (Supplementary Figure 1B). Notably, we found that all 11 of the detected lysophosphatidylcholine (LPC) species were increased in the N9 PTRF cells compared with the N9 cells, whereas 57% of the phosphatidylcholine (PC) species were significantly decreased in the N9 PTRF cells (Figure 1B, C). In addition to observing that increasing the amount of the PTRF protein significantly increased LPC levels while simultaneously decreasing PC levels, we found that increasing the PTRF level caused a significant increase in the accumulation of free fatty acids (Supplementary Figure 1C). These results clearly suggest that PTRF may substantially reprogram the phospholipid composition of GBM cells.

Given that our initial nontargeted LC-MS method is not optimized for lipid profiling, we next performed a focused lipidomics analysis (using both positive and negative ionization modes) to further characterize this PTRF-mediated phospholipid remodeling process (Supplementary Figure 1D). As expected, based on our lipidomics analysis, the N9 PTRF cells accumulated significantly higher levels of LPCs than did N9 cells (Figure 1D, E). The increased lipid-specific coverage afforded by this method enabled detection of 34 LPC species, among which 32 (94%) were accumulated to significantly higher levels in the N9 PTRF cells than in controls (Supplementary Figure 1E). To confirm that these observations were not an artifact of one specific cell line, we performed analysis based on enzyme-linked

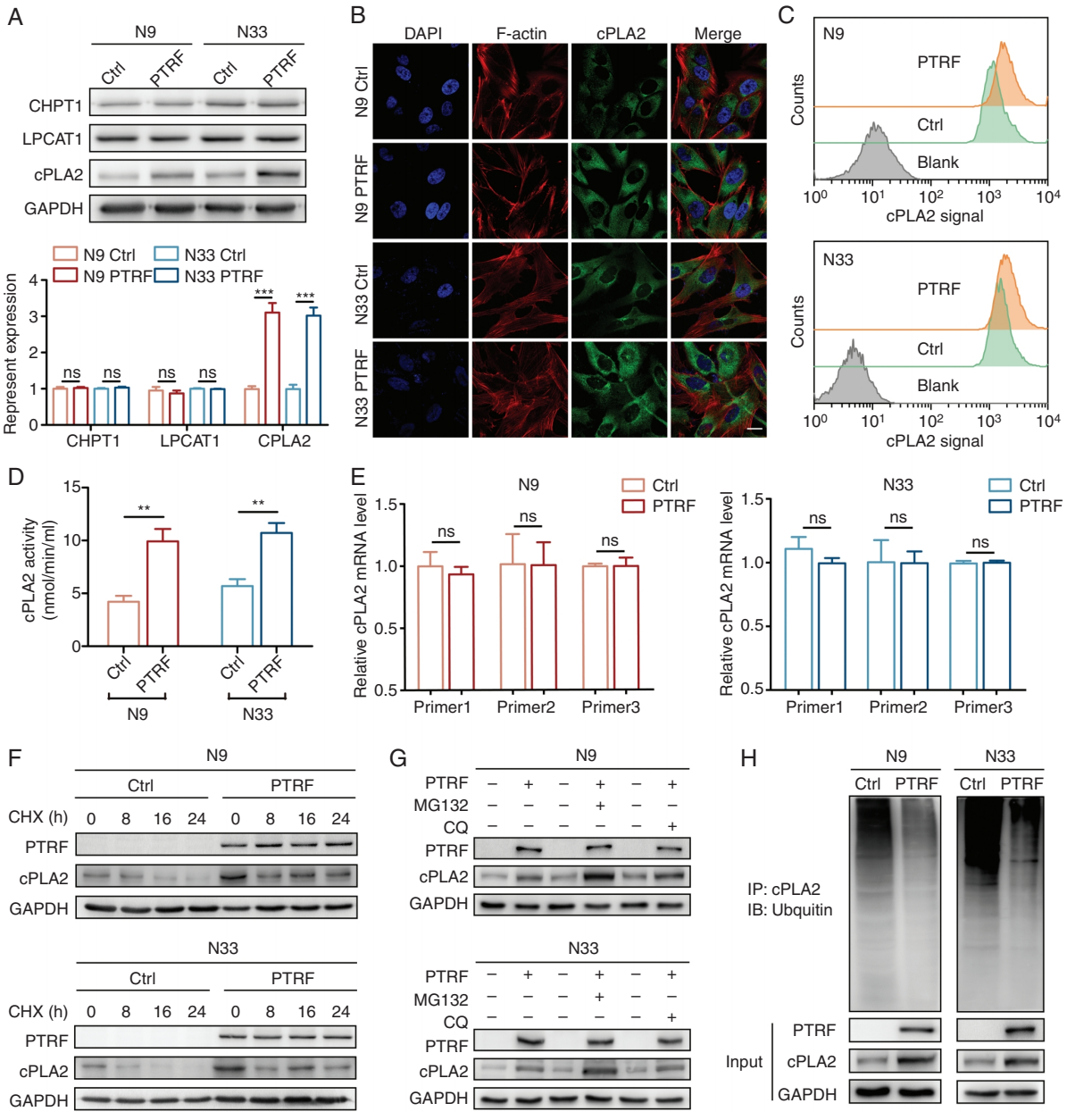

Fig. 2 PTRF reprograms phospholipid metabolism by regulating the stability of cPLA2. (A) Western blot analysis of CHPT1, LPCAT1, and cPLA2 expression in primary GBM cells (N9 and N33 cells transduced with vector or PTRF). Quantitation of the Western blot results using ImageJ software. (B) Immunofluorescence of cPLA2 (green), F-actin (red), and nuclei (blue). Scale bar, 20 μm. (C) Flow cytometry analysis of cPLA2 in GBM cells. (D) cPLA2 levels in GBM cells based on a cPLA2 assay kit. (E) Relative mRNA level of cPLA2, as determined by quantitative PCR. (F) Western blot analysis of cPLA2 and PTRF treated with cycloheximide (CHX) at the indicated time points. (G) Western blot analysis of cPLA2 and PTRF after treatment with the proteasome inhibitor MG132 or the lysosome inhibitor chloroquine (CQ). (H) GBM cells with or without PTRF overexpression were lysed and subjected to immunoprecipitation with an antibody against cPLA2 and analyzed by western blotting with an anti-ubiquitin antibody.

immunosorbent assay (ELISA) of total LPC levels in N9 and N33 cells and verified that the overall LPC levels were significantly higher in the cells overexpressing PTRF than in their respective control cells (Figure 1F). Collectively, these results indicate that PTRF somehow remodels lipid metabolism in GBM cells.

PTRF Reprograms Phospholipid Metabolism by Regulating the Stability of CPLA2

To explore the effects of PTRF on phospholipid remodeling, we immunoblotted N9 and N33 cells with antibodies against enzymes related to several lipid metabolic pathways,

including the Kennedy Pathway and Lands' cycle (eg, choline phosphotransferase 1 [CHPT1], lysophosphatidylcholine acyltransferase 1 [LPCAT1], and cPLA2) (Figure 2A and Supplementary Figure 2A). We detected a significant increase in the cPLA2 protein level in both N9 PTRF and N33 PTRF cells compared with their respective control cells. No differences were detected in CHPT1 and LPCAT1 protein levels. Moreover, both immunofluorescence assays and flow cytometry of N9 and N33 cells showed that the cPLA2 protein levels were significantly higher in cells overexpressing PTRF (Figure 2B, C). Note that analyses using a cytosolic phospholipase A2 assay kit and a secretory phospholipase A2 assay kit showed that the PTRF-overexpression-mediated increase in the cPLA2 level we observed in the N9 and N33 cells occurred independently of any alteration of secretory PLA2 (Figure 2D and Supplementary Figure 2B). We examined the cPLA2 protein by immunoblotting in the patient-derived GBM TBD0220 cells to determine its response to PTRF knockdown. The level of cPLA2 was significantly decreased by PTRF knockdown, and this decrease was reversed by reexpression of wild-type PTRF (Supplementary Figure 2C).

We next investigated how PTRF regulates cPLA2. Although we found that PTRF overexpression increased the cPLA2 level in N9 and N33 cells, we detected no correlation between PTRF and cPLA2 levels in the TCGA GBM database (Supplementary Figure 2D). Quantitative PCR analysis showed no significant changes in the mRNA level of cPLA2 between the N9 PTRF and N33 PTRF cells and their respective control cells, further suggesting the possibility of a posttranscriptional regulatory interaction (Figure 2E). To investigate whether PTRF somehow affects the stability of cPLA2, we used cycloheximide treatment to block protein synthesis. Immunoblotting showed that cPLA2 degradation occurred significantly faster in the control cells than in the N9 and N33 cells overexpressing PTRF (Figure 2F). Assays with a proteasome inhibitor (MG132) and a lysosome inhibitor (chloroquine) were performed in cultured GBM cells. We observed higher cPLA2 levels upon treatment with MG132 but not chloroquine (Figure 2G), indicating that cPLA2 was degraded via the proteasome-mediated degradation pathway. Further, staining with an antibody against ubiquitin revealed dramatically reduced ubiquitination of the cPLA2 protein in the cells overexpressing PTRF compared with control cells (Figure 2H), suggesting that PTRF promotes the stability of cPLA2 by somehow inhibiting its proteasome-mediated degradation.

PTRF Increases the Endocytosis Capacity of GBM Cells by Promoting LPC-Mediated Increases in Membrane Fluidity

Changes in the composition of phospholipids can alter the properties of cell membranes, thereby affecting cell membrane functions.[17] To test the relationship between PTRF and cell membrane fluidity, we used FRAP analysis with CLSM. The fluorescence recovery of the cells overexpressing PTRF was significantly faster than that of control cells (Figure 3A, B). Considering our findings from the aforementioned lipidomics analysis, we supplemented the membranes of control cells with a mixture of LPCs, which increased the speed of fluorescence recovery. We also conducted standard experiments with fluorescent probes to detect relative membrane fluidity, which showed that both PTRF overexpression and LPC supplementation increased membrane fluidity (Figure 3C). Together, these results indicate that PTRF may increase cell membrane fluidity by increasing the LPC content in the plasma membranes of GBM cells.

To help clarify the function of this PTRF-cPLA2 lipid remodeling pathway in regulating membrane fluidity, we revisited our initial correlation analysis data for the PTRF-related genes from the public cancer databases. Gene Ontology enrichment analysis indicated enrichment of endocytosis among the PTRF-related genes (Supplementary Figure 3A), and GSEA indicated enrichment of endocytosis and positive regulation of endocytosis terms among the patients with high PTRF levels (Supplementary Figure 3B). These results suggesting altered dynamics for endocytosis-related genes were conspicuous in light of the known impacts of both differential membrane lipid content and cell membrane fluidity on this active transport process.

We next used Cy5-labeled bovine serum albumin (BSA) to detect endocytosis in GBM cells. Immunofluorescence analysis by CLSM was used to directly observe the endocytosis of Cy5-BSA after 4 h of incubation with N9 and N33 cells. The N9 PTRF and N33 PTRF cells had significantly stronger fluorescence intensity than the respective control cells, indicating that activating the PTRF-cPLA2 lipid remodeling pathway may increase endocytosis capacity (Supplementary Figure 3C). Quantitation based on flow cytometry analysis confirmed this result (Figure 3D and Supplementary Figure 3D). We also conducted a flow cytometry–based time curve (1–8 h) analysis of Cy5-BSA uptake into N9 and N33 cells, which showed that the endocytosis rate was significantly increased in N9 PTRF and N33 PTRF cells compared with controls (Figure 3E). Further, we found that the fluorescence intensity of Cy5-BSA was significantly decreased in TBD0220 cells with PTRF knockdown compared with controls (Supplementary Figure 3E). Thus, the PTRF-cPLA2 lipid remodeling pathway can apparently enhance both the quantity and the rate of endocytosis in GBM cells.

The PTRF-cPLA2 Lipid Remodeling Pathway Regulates Mitochondrial Respiration and Cell Proliferation in GBM

Previous in vitro studies have confirmed that fatty acids provided by cPLA2 support energy generation via fatty acid oxidation in mitochondria.[18,19] To verify whether the PTRF-cPLA2 lipid remodeling pathway alters energy metabolism in GBM cells, we performed a mitochondrial stress test using a Seahorse Extracellular Flux Analyzer. Dynamic tracking showed that overexpression of PTRF significantly increased the OCR in both tested cell lines compared with controls (Figure 3F). This analysis also showed that overexpression of PTRF increased basal respiration, proton leakage, and ATP production in N9 and N33 cells (Figure 3G–I). We confirmed the expected increase in the intracellular ATP concentration in N9 PTRF and N33 PTRF

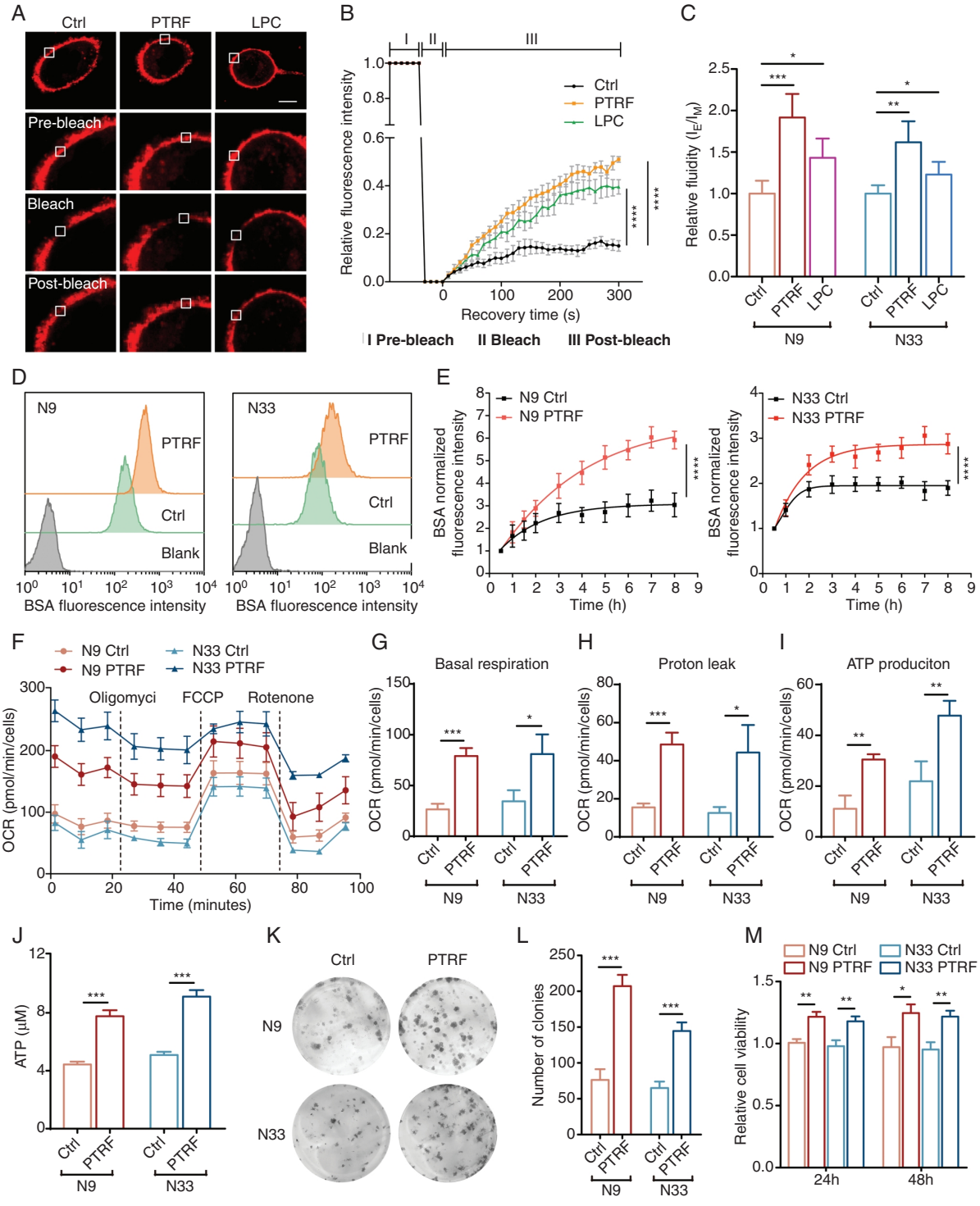

Fig. 3 The PTRF-cPLA2 lipid remodeling pathway regulates the endocytosis capacity, mitochondrial respiration, and proliferation of GBM cells. (A) Confocal images from a FRAP assay showing plasma membrane fluidity changes in N9 and N9 PTRF cells, as well as in N9 cells treatment with an exogenous LPC. Scale bar, 10 μm. (B) Plot showing the fluorescence recovery of the cells in (A). (C) Pyrene assay showing the relative membrane fluidity of GBM cells. (D) Flow cytometry analysis of GBM cells after incubation with Cy5-BSA for 4 h. (E) Flow cytometry-based time curve (1–8 h) for GBM cells after incubation with Cy5-BSA. (F) Time series for the OCR measurements of GBM cells using a Seahorse Analyzer. $n = 3$–4 replicates per group. (G–I) OCR measurements of basal respiration (G), proton leakage (H), and ATP production (I) in GBM cells. (J) Direct measurement of the intracellular ATP concentration by bioluminescence. (K) Colony formation assay was performed in GBM cells. (L) Quantification of colony numbers in (K). (M) Relative cell viability of GBM cells.

cells (Figure 3J), while the ATP concentration decreased in TBD0220 cells with PTRF knockdown (Supplementary Figure 3F). Further, PTRF overexpression promotes both the colony formation and the proliferative capacities of GBM cells (Figure 3K–M, while PTRF knockdown suppresses these capacities (Supplementary Figure 3G–I).

A cPLA2 Inhibitor Represses Endocytosis, ATP Production, and GBM Cell Proliferation Through Suppressing PTRF-Mediated Phospholipid Reprogramming

Given our finding that PTRF promotes cPLA2 stability and our general observation in the laboratory that the N9 PTRF and N33 PTRF cells grew at obviously higher rates than their respective controls, we next conducted a series of inhibitor assays to explore a possible oncogenic function for cPLA2. The cPLA2 inhibitor arachidonyl trifluoromethyl ketone (AACOCF3) is a selective slow binding inhibitor of cPLA2 (Figure 4A). Compared with the DMSO controls, the N9 PTRF and N33 PTRF cells treated with AACOCF3 had significantly decreased total LPC levels (Supplementary Figure 4A).

Lipidomics also showed that 9 types of LPC decreased by 33% after AACOCF3 treatment (Figure 4B and Supplementary Figure 4B), indicating that blocking the phospholipase activity of cPLA2 can partially reverse the PTRF overexpression–induced remodeling of GBM cells. We also conducted assays that showed that AACOCF3 treatment decreased BSA uptake (Figure 4C and Supplementary Figure 4C). These results confirmed that cPLA2 participates in the PTRF-induced remodeling of GBM cells and showed that the metabolic contribution of cPLA2 to this remodeling affects membrane uptake properties.

We used the Seahorse apparatus to investigate the role of cPLA2 in PTRF-induced alterations in GBM energy metabolism and found that AACOCF3 treatment significantly decreased the OCR of the N9 and N33 cells (Figure 4D, E). These analyses revealed that AACOCF3 treatment also decreased basal respiration, proton leakage, and ATP production in both N9 and N33 cells (Figure 4F–H). We also detected significantly decreased intracellular ATP concentrations in tumor cells treated with AACOCF3 (Figure 4I). Cell proliferation (Figure 4L) and colony formation assays (Figure 4J and Supplementary Figure 4D) showed that AACOCF3 treatment inhibited GBM cell proliferation in vitro. In summary, these results indicate that PTRF reprograms phospholipid metabolism via cPLA2 and show that the PTRF-induced and cPLA2-mediated ability to promote tumor cell proliferation is blocked by inhibiting the phospholipase catalytic function of cPLA2.

PTRF Promotes GBM Tumor Proliferation and Suppresses Immune Responses In Vivo

To further investigate the impacts of the PTRF-cPLA2 lipid remodeling pathway in vivo, we established an intracranial GBM PDX model in BALB/c nude mice (Figure 5A). As assessed via bioluminescence imaging on days, PTRF overexpression resulted in a significant increase in tumor growth (Figure 5B, C). Kaplan–Meier survival curves indicated that the mice bearing PTRF-overexpressing tumors had worse survival than controls (Figure 5D). HE staining of tumors confirmed a significant increase in tumor burden in the PTRF group compared with the control group (Figure 5E). IHC staining showed that overexpression of PTRF was accompanied by high expression of Ki-67, indicating that overexpression of PTRF increased cell proliferation, which is consistent with the bioluminescence and HE results (Figure 5F and Supplementary Figure 5A), and that the ATP levels were significantly higher in the PTRF-overexpressing tumor cells (Supplementary Figure 5B). We investigated the effects in an orthotopic mouse model by transducing small interfering PTRF-1 lentivirus into TBD0220 cells. Bioluminescence imaging and HE staining showed significantly slower growth of the tumor upon PTRF knockdown (Supplementary Figure 5C, D), and Kaplan–Meier survival curves indicated that mice with PTRF-knockdown tumors had a better prognosis (Supplementary Figure 5E).

Tumor growth relies not only on the ATP levels of the tumor cells but also on tumor immunosuppression by extracellular ATP and purinergic signaling. To investigate the role of PTRF and energy metabolism in the tumor microenvironment, we established a GL261 intracranial tumor model in C57BL/6 mice to examine the adenosinergic pathway (extracellular purinergic signaling) (Figure 5G). In the adenosinergic pathway, extracellular ATP is converted to adenosine by the enzymes CD39 and CD73. We measured the levels of ATP and adenosine in the tumor microenvironment of the intracranial tumor model and found that PTRF overexpression significantly increased the extracellular levels of both compounds (Figure 5H, I). Publicly available single-cell RNA sequencing data also demonstrated that CD39 and CD73 are highly expressed in GBM tumor cells (Supplementary Figure 5F).

To evaluate the capability of PTRF to suppress immune responses, the levels of interferon gamma (IFN-γ) and granzyme B (GrB) in the tumors were measured. The overexpression of PTRF significantly reduced the levels of IFN-γ (Supplementary Figure 5G) and GrB (Figure 5J). Furthermore, tumor-infiltrating lymphocytes (TILs) were analyzed by flow cytometry, and the results showed that low levels of CD8+ TILs were observed in the PTRF-overexpressing tumors (Figure 5K and Supplementary Figure 5H). As antitumor immunity is typically accompanied by apoptosis of tumor tissues, we used assays by TUNEL (terminal deoxynucleotidyl transferase deoxyuridine triphosphate nick end labeling) to examine the apoptosis levels in tumor tissues. Tumor tissues from the control mice exhibited extensive apoptosis, whereas only a small number of apoptotic cells were detected in the tumor tissues from PTRF overexpression mice (Supplementary Figure 5I). Taken together, these results suggest that the PTRF-cPLA2 lipid remodeling pathway may induce immunosuppressive effects, possibly by providing fuel to activate the adenosinergic pathway.

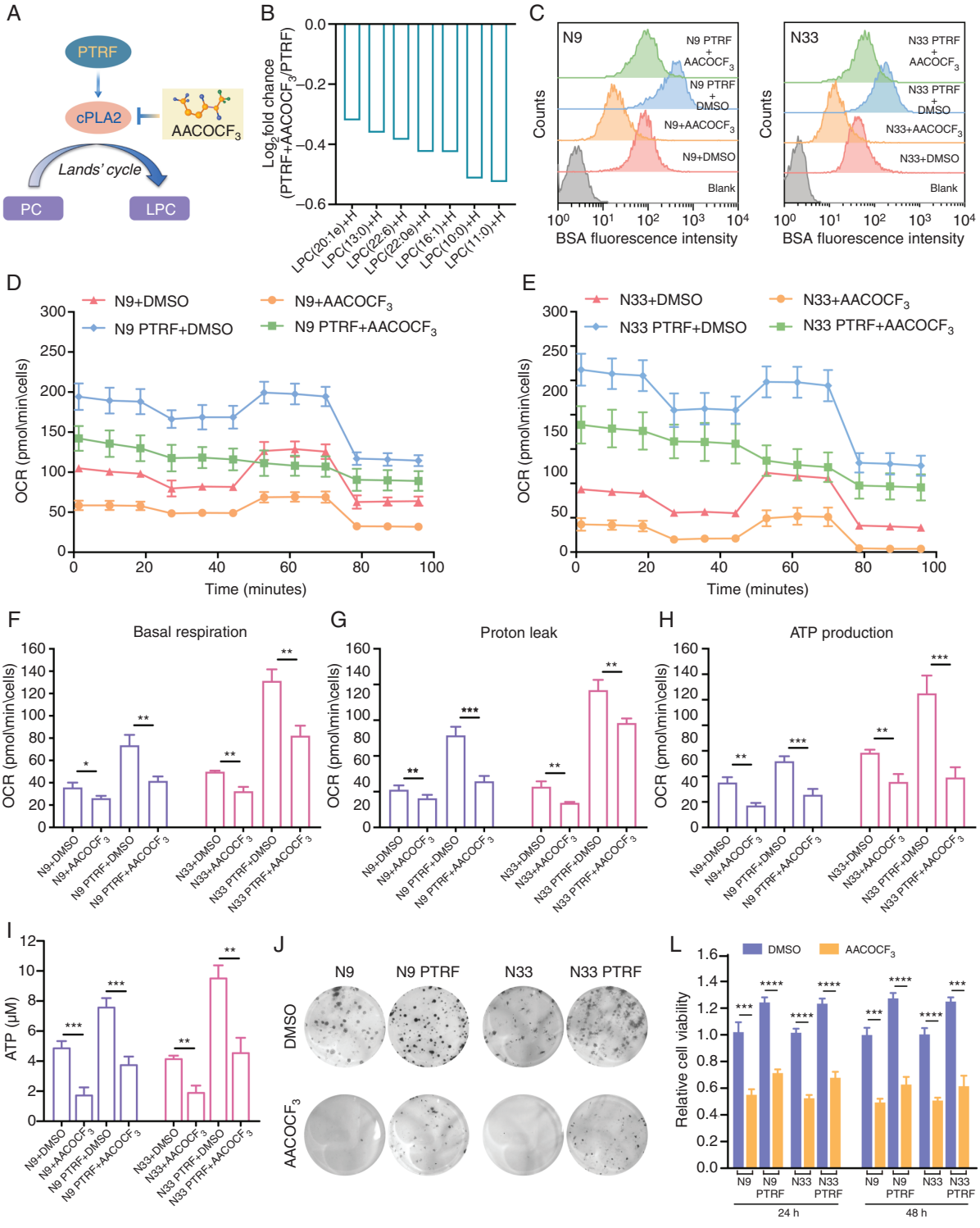

Fig. 4 A cPLA2 inhibitor represses endocytosis, ATP production, and GBM cell proliferation through suppressing PTRF-mediated phospholipid reprogramming. (A) Schematic model of the role of cPLA2 in PTRF-induced phospholipid remodeling. (B) Fold change in the levels of various LPCs in N9 PTRF cells treated with DMSO or $AACOCF_3$ based on lipidomics analysis. (C) Flow cytometry analysis of Cy5-BSA after 4 h incubation with DMSO or AACOCF3. (D) N9 cells with or without PTRF overexpression were seeded in XF24 well plates, and treated with DMSO or AACOCF3 for bioenergetic measurements. $n = 3$–4 replicates per group. (E) N33 cells with or without PTRF overexpression were seeded in XF24 well plates, and treated with DMSO or AACOCF3 for bioenergetic measurements. $n = 3$–4 replicates per group. (F–H) Graphs showing basal respiration (F), proton leakage (G), and ATP production (H) of GBM cells treated with DMSO or AACOCF3. (I) Intracellular ATP concentration in GBM cells treated with DMSO or AACOCF3, as detected via bioluminescence. (J) Colony formation of GBM cells treated with DMSO or AACOCF3. (K) Relative cell viability of GBM cells treated with DMSO or AACOCF3.

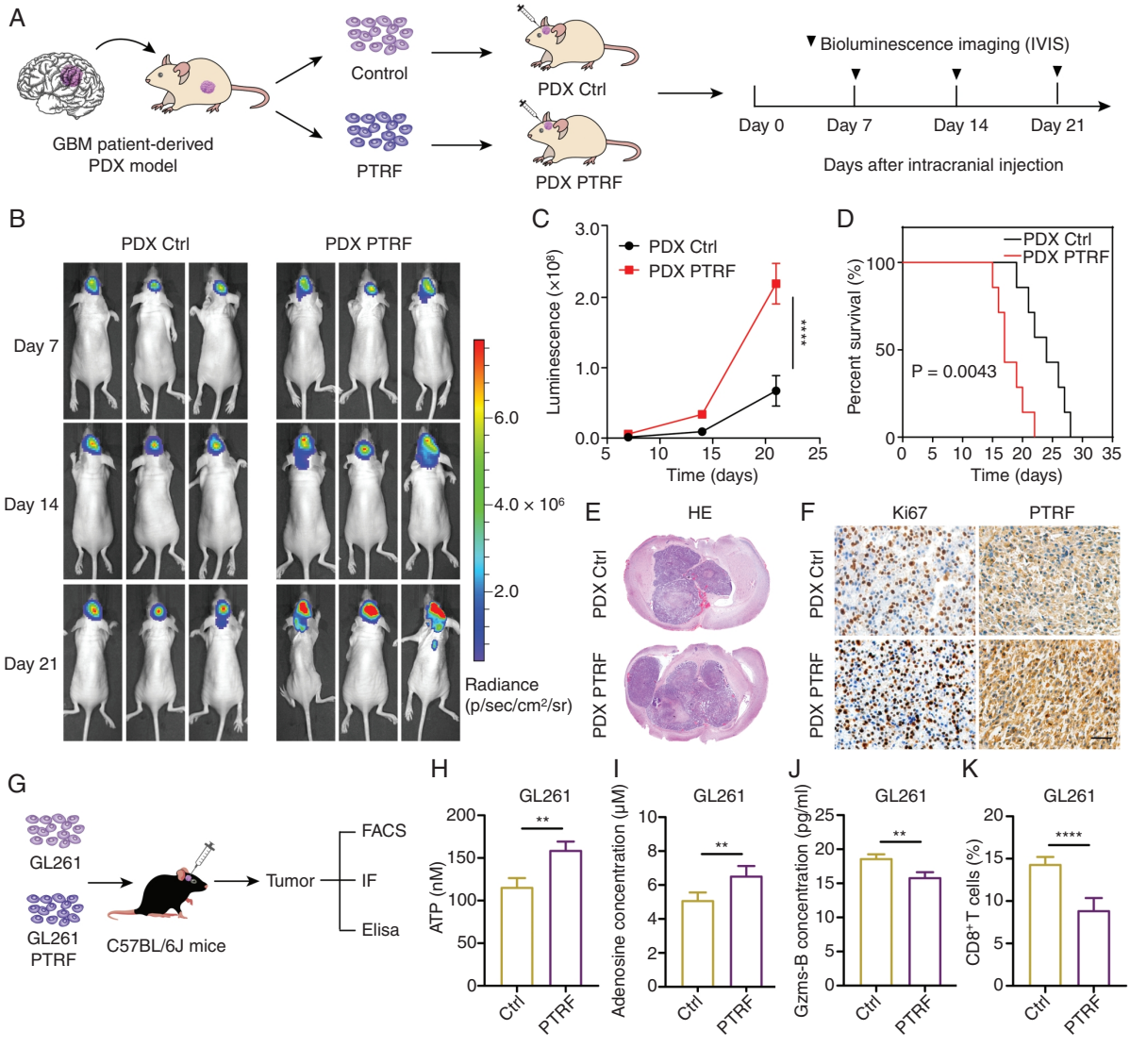

Fig. 5 PTRF promotes GBM tumor proliferation and suppresses immune responses in vivo. (A) Schematic of the overexpression of PTRF in patient-derived GBM orthotopic xenograft model using lentivirus vector ($n = 7$ for each group). (B) Representative tumor bioluminescence images of mice at 7, 14, and 21 days after tumor implantation. (C) Tumor growth curves for mice by quantification of bioluminescent imaging signal intensities. (D) Kaplan–Meier survival curve of nude mice. (E) Representative images of H&E staining for tumor volume in the nude mice. (F) IHC staining for Ki-67 and PTRF in the samples. Scale bar, 50 μm. (G) Schematic of the GL261 intracranial tumor model used to investigate the role of PTRF in the immune microenvironment. (H) The levels of ATP in the tumor microenvironment of control and PTRF-overexpressing intracranial tumor model mice. (I) The levels of adenosine in the tumor microenvironment. (J) The levels of GrB within the tumors. (K) Flow cytometry analysis of CD8+ T cells (gated on CD45+CD3+ cells) within GL261 tumors. $n = 5$–6, with each sample representing tumor tissue from one mouse.

AACOCF3 + Metformin as Combination Therapy Against GBM

Seeking new treatment modalities for GBM patients with a high PTRF level, we next used intracranial PDX models with PTRF-overexpressing tumors and tested both monotherapies and combination therapy with the cPLA2 inhibitor AACOCF3 and metformin, a drug that reduces ATP synthesis (Supplementary Figure 6A). Compared with vehicle, both the AACOCF3 and metformin monotherapies significantly reduced the growth of the tumor (Figure 6A, C) and significantly increased survival rates (Figure 6B). Moreover, the combination therapy had further significant effects on both tumor growth reduction and increased survival rates. IHC staining of tumor sections showed that all the therapies reduced the levels of Ki-67, with the combination therapy again showing the most pronounced reductions (Figure 6D and Supplementary Figure 6B). In addition, the cellular ATP levels in the tumor tissues were reduced (Supplementary Figure 6C).

We further examined whether AACOCF3, metformin, and/or a combination of these inhibitors can relieve the

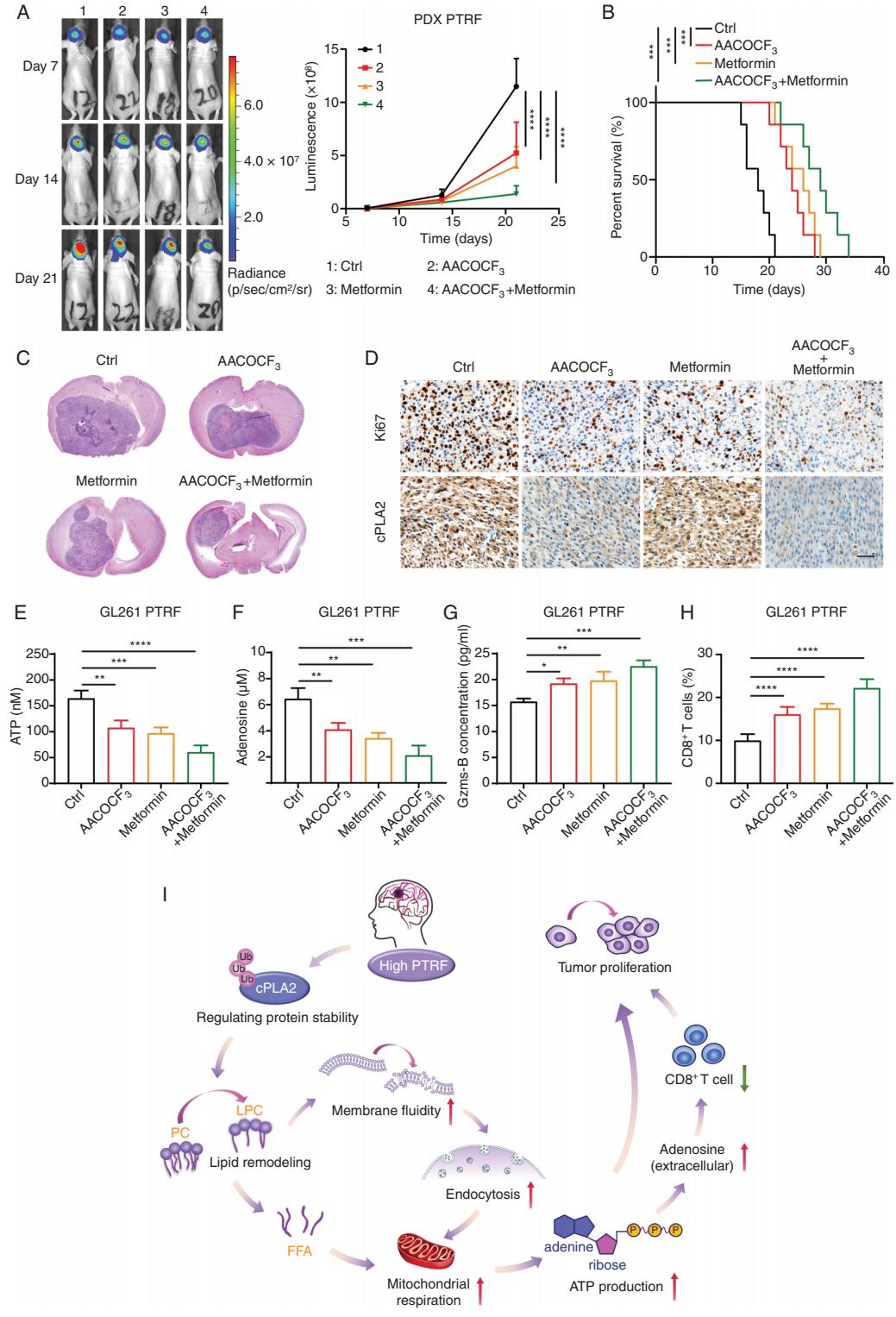

Fig. 6 AACOCF3 and metformin as a combination therapy against GBM. (A) Representative tumor bioluminescence images of nude mice at 7, 14, and 21 days after tumor implantation. Tumor growth curves for mice bearing PTRF-overexpressing tumors and treated with AACOCF3, metformin, or a combination of AACOCF3 and metformin by quantification of bioluminescence imaging signal intensities ($n = 7$ for each group). (B) Kaplan–Meier survival curves of the nude mice. (C) Representative images of HE staining of tumors from the nude mice. (D) IHC staining for Ki-67 and cPLA2 in the samples. Scale bar, 50 μm. (E) The levels of ATP in the tumor microenvironment of GL261 tumor with PTRF overexpression in mice treated with AACOCF3, metformin, or a combination of AACOCF3 and metformin. (F) The levels of adenosine in the tumor microenvironment. (G) The levels of GrB within GL261 tumors with PTRF overexpression in mice treated with the indicated agents. (H) Flow cytometry analysis of CD8+ T cells. $n = 5$, with each sample representing tumor tissue from one mouse. (I) The mechanistic scheme by which PTRF remodels phospholipid metabolism to promote tumor proliferation and suppress immune responses in glioblastoma by stabilizing cPLA2.

effect of PTRF on suppressing immune responses in GBM (Supplementary Figure 6D). The ATP and adenosine levels were significantly reduced in the tumor microenvironment of the AACOCF3 and metformin monotherapy group (Figure 6E, F). Furthermore, the AACOCF3 and metformin monotherapies both increased the levels of IFN-γ (Supplementary Figure 6E) and GrB (Figure 6G), increased CD8+ TILs (Figure 6H and Supplementary Figure S6F), and increased the extent of apoptosis in tumor tissues (Supplementary Figure 6G). We again found that the combination therapy outperformed either of the monotherapies for all of the tested parameters, highlighting its strong potential as a novel approach for the treatment of GBM.

Discussion

In this study, we found that PTRF remodeled phospholipids through cPLA2 to promote tumor proliferation and immune suppression in GBM (Figure 6I). The tumor-promoting effect of PTRF in gliomas is widely recognized; previous studies have shown PTRF protects vascular endothelial cells from cytotoxic C lymphocyte–mediated cell death[20] and that a partial loss of PTRF causes potent immune responses in the challenge phase of asthma.[21] In GBM, PTRF is negatively correlated with the number of cytotoxic lymphocytes by bioinformatics analyses.[16] Consistently, our data showed a reduction in the CD8+ TILs in tumor tissues with PTRF overexpression, indicating that PTRF suppresses immune responses in GBM.

Metabolic reprogramming is a hallmark of cancer. Tumor-related metabolic alterations cover all stages of cell-metabolite interactions, including the ability to obtain the necessary nutrients and to use these nutrients to generate energy and build new biomass.[5,22] Tumor cells can take in macromolecular substances such as polysaccharides, fatty acids, and protein. Palm et al suggested that cancer cells can use endocytosis to internalize extracellular proteins and degrade them in lysosomes, providing an important source of intracellular amino acids.[23] We found that the PTRF-cPLA2 lipid remodeling pathway promotes GBM survival by enhancing endocytosis and energy metabolism. Elevation of LPC levels by PTRF can alter the fluidity of the cell membrane and thereby increase the uptake of extracellular macromolecular nutrients, indicating that phospholipid remodeling can enhance endocytosis. All living cells rely on the uptake of nutrients, which are then directed into multiple metabolic pathways to generate energy. Our results also suggest that the endocytosis pathway might participate in cellular energy metabolism, but the mechanism is unclear.

Cytoplasmic PLA2 hydrolyzes the fatty acyl chain of phospholipids at the sn-2 position to produce lysophospholipids and fatty acids. Slatter et al showed that lipid membrane remodeling is necessary to support energy requirements during platelet activation; they found that cPLA2 has a previously unrecognized biological function in metabolism, through which it serves as a regulator of mitochondrial energy production.[19] Consistently, we found that cPLA2-mediated phospholipid remodeling can promote mitochondria energy metabolism.

As a direct source of cell energy, ATP can provide support for cell biological activities. Among these activities, the effect of ATP on tumor cell proliferation has been widely recognized in many tumors. Our study revealed that increased ATP levels strongly promote the proliferation of GBM cells in vitro and in vivo. In addition to the effects on the tumor itself, ATP can affect the tumor cell microenvironment. Large-scale research efforts have been focused on selectively targeting cellular ATP metabolic pathways, with emphasis on extracellular purinergic signaling.[24] Adenosine is an important factor produced by cancer cells and immune cells in the tumor microenvironment that can inhibit antitumor responses. Adenosine can be produced via the catalysis of ATP by proteins, including CD73 and CD39, that are expressed on the cell surface. The inhibitory effect of adenosine on the antitumor response has been demonstrated in many studies, and a variety of treatments based on adenosine metabolism[25]—for example, by blocking adenosine receptors through specific antagonists—have been developed. There are also efforts to develop immunotherapies that target CD73 and CD39,[26] and CD73 in particular has been identified as a target for specific immunotherapy in GBM, offering improved antitumor immune responses for GBM during immune checkpoint therapy.[27] In this context, in addition to demonstrating the functional contributions of PTRF-induced phospholipid remodeling to nutritional endocytosis, fatty acid oxidation in mitochondria, ATP, adenosine metabolism, and the suppression of tumor immune responses, our study has defined multiple new targets for developing GBM therapies specifically and perhaps adenosine-related immunotherapies more generally.

Supplementary Material

Supplementary data are available online at *Neuro-Oncology* (http://neuro-oncology.oxfordjournals.org/).

Keywords

cPLA2 | energy metabolism | glioblastoma | phospholipid remodeling | PTRF

Funding

This work was supported by the National Natural Science Foundation of China (NSFC, no. 81772667), the Beijing Tianjin Hebei Basic Research Cooperation Project (nos. 18JCZDJC45500 and H2018201306), and the Tianjin Key R&D Plan of Tianjin Science and Technology Plan Project (no. 20YFZCSY00360).

Conflict of interest statement. The authors declare no conflicts of interest.

Authorship statement. Developed the study concept and designed the study: CSK and KKY. Conducted the experiments and acquired the data: KKY, QZ, QXW, CF, YLT, YFW, JHZ, CY, and YSL. Analyzed the data, generated the figures, and wrote the paper: KKY and QZ. Funded the work and provided overall research supervision: CSK. Approved the final manuscript: All authors.

References

1. Ostrom QT, Gittleman H, Liao P, et al. CBTRUS statistical report: primary brain and other central nervous system tumors diagnosed in the United States in 2010–2014. *Neuro Oncol.* 2017;19(suppl_5):v1–v88.
2. Van Meir EG, Hadjipanayis CG, Norden AD, Shu HK, Wen PY, Olson JJ. Exciting new advances in neuro-oncology: the avenue to a cure for malignant glioma. *CA Cancer J Clin.* 2010;60(3):166–193.
3. Lyssiotis CA, Kimmelman AC. Metabolic interactions in the tumor microenvironment. *Trends Cell Biol.* 2017;27(11):863–875.
4. Agnihotri S, Zadeh G. Metabolic reprogramming in glioblastoma: the influence of cancer metabolism on epigenetics and unanswered questions. *Neuro Oncol.* 2016;18(2):160–172.
5. Pavlova NN, Thompson CB. The emerging hallmarks of cancer metabolism. *Cell Metab.* 2016;23(1):27–47.
6. Bi J, Ichu TA, Zanca C, et al. Oncogene amplification in growth factor signaling pathways renders cancers dependent on membrane lipid remodeling. *Cell metabolism.* 2019;30(3):525–538 e528.
7. Wang B, Rong X, Palladino END, et al. Phospholipid remodeling and cholesterol availability regulate intestinal stemness and tumorigenesis. *Cell Stem Cell.* 2018;22(2):206–220.e4.
8. Morita Y, Sakaguchi T, Ikegami K, et al. Lysophosphatidylcholine acyltransferase 1 altered phospholipid composition and regulated hepatoma progression. *J Hepatol.* 2013;59(2):292–299.
9. Fack F, Tardito S, Hochart G, et al. Altered metabolic landscape in IDH-mutant gliomas affects phospholipid, energy, and oxidative stress pathways. *EMBO Mol Med.* 2017;9(12):1681–1695.
10. Hill MM, Bastiani M, Luetterforst R, et al. PTRF-cavin, a conserved cytoplasmic protein required for caveola formation and function. *Cell.* 2008;132(1):113–124.
11. Liu L, Brown D, McKee M, et al. Deletion of Cavin/PTRF causes global loss of caveolae, dyslipidemia, and glucose intolerance. *Cell Metab.* 2008;8(4):310–317.
12. Patni N, Garg A. Congenital generalized lipodystrophies—new insights into metabolic dysfunction. *Nat Rev Endocrinol.* 2015;11(9):522–534.
13. Huang K, Fang C, Yi K, et al. The role of PTRF/Cavin1 as a biomarker in both glioma and serum exosomes. *Theranostics.* 2018;8(6):1540–1557.
14. Wang W, Zhao Z, Wu F, et al. Bioinformatic analysis of gene expression and methylation regulation in glioblastoma. *J Neurooncol.* 2018;136(3):495–503.
15. Wang Z, Tang W, Yuan J, Qiang B, Han W, Peng X. Integrated analysis of RNA-binding proteins in glioma. *Cancers (Basel).* 2020;12(4):892.
16. Guo Q, Guan GF, Cheng W, et al. Integrated profiling identifies caveolae-associated protein 1 as a prognostic biomarker of malignancy in glioblastoma patients. *CNS Neurosci Ther.* 2019;25(3):343–354.
17. Harayama T, Riezman H. Understanding the diversity of membrane lipid composition. *Nat Rev Mol Cell Biol.* 2018;19(5):281–296.
18. Lue HW, Podolak J, Kolahi K, et al. Metabolic reprogramming ensures cancer cell survival despite oncogenic signaling blockade. *Genes Dev.* 2017;31(20):2067–2084.
19. Slatter DA, Aldrovandi M, O'Connor A, et al. Mapping the human platelet lipidome reveals cytosolic phospholipase A2 as a regulator of mitochondrial bioenergetics during activation. *Cell Metab.* 2016;23(5):930–944.
20. Thommen DS, Schuster H, Keller M, et al. Two preferentially expressed proteins protect vascular endothelial cells from an attack by peptide-specific CTL. *J Immunol.* 2012;188(11):5283–5292.
21. Ni Y, Hao J, Hou X, et al. Dephosphorylated polymerase I and transcript release factor prevents allergic asthma exacerbations by limiting IL-33 release. *Front Immunol.* 2018;9:1422.
22. DeBerardinis RJ, Chandel NS. Fundamentals of cancer metabolism. *Sci Adv.* 2016;2(5):e1600200.
23. Palm W, Park Y, Wright K, Pavlova NN, Tuveson DA, Thompson CB. The utilization of extracellular proteins as nutrients is suppressed by mTORC1. *Cell.* 2015;162(2):259–270.
24. Di Virgilio F, Sarti AC, Falzoni S, De Marchi E, Adinolfi E. Extracellular ATP and P2 purinergic signalling in the tumour microenvironment. *Nat Rev Cancer.* 2018;18(10):601–618.
25. Boison D, Yegutkin GG. Adenosine metabolism: emerging concepts for cancer therapy. *Cancer Cell.* 2019;36(6):582–596.
26. Young A, Mittal D, Stagg J, Smyth MJ. Targeting cancer-derived adenosine: new therapeutic approaches. *Cancer Discov.* 2014;4(8):879–888.
27. Goswami S, Walle T, Cornish AE, et al. Immune profiling of human tumors identifies CD73 as a combinatorial target in glioblastoma. *Nat Med.* 2020;26(1):39–46.